Journal of Science and Transport Technology
Journal homepage: https://jstt.vn/index.php/en

Enhancing Combustion Characteristics of Ammonia-Fueled Motorcycle Engines using Multi-Point Ignition Strategy

Bui Van Hung[1], Le Khac Binh[2*], Tran Minh Ho[3]
[1]Danang University of Technology and Education, The University of Danang, Vietnam
[2]Vinh University of Technology Education, Vietnam
[3]Dong A University, Vietnam

Article info
Type of article:
Original research paper

DOI:
https://doi.org/10.58845/jstt.utt.2026.en.6.2.277-296

***Corresponding author:**
Email address:
khacbinhktv@gmail.com

Received: 18/12/2025
Received in Revised Form: 29/03/2026
Accepted: 14/04/2026

Abstract: This study presents simulation results on the influence of ignition system configuration on the performance and emissions of an ammonia-fueled motorcycle engine. Two ignition strategies were examined on a Honda engine at 7500 rpm: single-point ignition and three-point distributed ignition. The results indicate that the single-spark configuration failed to overcome ammonia's low laminar flame speed, resulting in a power output of only 4.36 kW (32% lower than that of gasoline). In contrast, the three-spark system significantly enhanced combustion rates, elevating peak pressure to 45.49 bar (exceeding the gasoline baseline of 41.39 bar) and increasing power to 5.36 kW. Although the three-point configuration increased NOx emissions to 908 ppm at an ignition timing of 30°CA, retarding the timing to 20°CA reduced NOx to 294 ppm while maintaining a power output of 4.83 kW. The findings confirm that multi-point ignition, combined with MBT (Minimum advance for Best Torque) optimization for each ignition configuration, is essential for the practical application of NH_3 in high-speed motorcycle engines.

Keywords: Ammonia fuel; Spark ignition engine; Multi-point ignition; NOx emissions; Motorcycle engine.

1. Introduction

In the context of escalating global climate change and increasingly stringent environmental regulations, the search for sustainable alternative energy sources to mitigate dependency on fossil fuels has become an urgent priority. Ammonia (NH_3) is emerging as one of the most promising candidates, widely recognized as a viable carbon-free fuel solution with immense application potential for internal combustion engines (ICEs), the maritime sector, and power generation [1-3].

The fundamental advantage of ammonia lies in its carbon-free molecular structure. Theoretically, the complete combustion of ammonia releases only nitrogen (N_2) and water vapor (H_2O), effectively eliminating CO_2 emissions at the source [4-6]. Therefore, ammonia serves as a potential carbon-neutral fuel, playing a pivotal role in achieving the Net-Zero emissions target by 2050 [7-9]. Beyond its utility as a direct fuel, ammonia is also considered an effective hydrogen carrier, addressing the technical barriers currently encountered by the hydrogen economy [10-11].

Although hydrogen is considered an ideal clean fuel, challenges regarding storage and transportation-stemming from its low volumetric

energy density and extreme liquefaction temperature requirements (-253°C)-have hindered its widespread adoption. In this context, ammonia exhibits significant superiority. With a hydrogen content of 17.8% by mass, ammonia possesses a hydrogen density approximately 50% higher than that of compressed or liquefied hydrogen [12-13]. Specifically, the volumetric energy density of liquid ammonia (approximately 13.72 MJ/m³ or 7.1 MJ/L) is about 1.7 times higher than that of liquid hydrogen [14-16]. Regarding operational characteristics, ammonia boasts a superior research octane number (RON) of 130, significantly higher than that of commercial gasoline (90-98) [17]. This attribute makes it an excellent anti-knock fuel, allowing spark-ignition engines to operate at substantially higher compression ratios (up to 15-16:1) to maximize thermal efficiency without concerns about pre-ignition or destructive knocking [18]. In practice, especially under high-load conditions, the presence of ammonia enables the optimization of ignition timing (by advancing the ignition phase) instead of retarding it to avoid knocking, as in gasoline engines, thereby enhancing the combustion process and improving the indicated thermal efficiency [19].

More importantly, ammonia can be easily liquefied at relatively low pressures (approximately 10 bar) at ambient temperature or at -33°C under atmospheric pressure [20]. This physical characteristic renders the storage and transportation of ammonia significantly safer, simpler, and more economical compared to hydrogen. Studies indicate that the cost of storing hydrogen in the form of ammonia is only about one-third of that for pure hydrogen storage, and the total transportation costs can be 10.6 to 30.2 times lower [6, 21]. Consequently, ammonia is regarded as the most efficient hydrogen storage and distribution medium currently available; it can be utilized directly or cracked back into hydrogen at the point of consumption through catalytic processes [22-24].

Another major competitive advantage of ammonia is the availability of existing global infrastructure. As one of the world's most widely produced and transported chemicals for the fertilizer industry, ammonia already benefits from a comprehensive logistics network, including port systems, storage facilities, pipelines, and standardized safety protocols [25-27]. Leveraging this existing infrastructure significantly minimizes the initial capital investment required for the transition to an ammonia-based energy economy, providing a level of flexibility that other emerging alternative fuels lack.

Despite its storage advantages, ammonia is considered a 'challenging' fuel for engine combustion due to its low chemical reactivity. Ammonia has an auto-ignition temperature of approximately 651°C (924K), which is significantly higher than that of diesel (approximately 210°C) and gasoline (approximately 260°C) [6]. This presents substantial hurdles for cold starting and necessitates extremely high compression ratios (potentially up to 35:1 or higher) if utilized in compression-ignition engines without auxiliary assistance [28]. The laminar burning velocity of ammonia is exceptionally slow, measuring only about 6-8 cm/s (0.06-0.08 m/s) under ambient conditions-far lower than that of gasoline (approximately 40-60 cm/s) and hydrogen (approximately 200-300 cm/s) [29]. This low burning rate leads to a prolonged, less stable combustion process that is prone to quenching, particularly at high engine speeds [30]. To initiate combustion, ammonia requires a minimum ignition energy that is much higher than that of conventional hydrocarbon fuels [31]. Simultaneously, its narrow flammability limits further restrict the engine's stable operating window [32].

Beyond thermodynamic characteristics, safety is a critical factor to consider. Ammonia is highly toxic and exhibits strong corrosivity toward

certain materials, such as copper, zinc, and their alloys [33-34]. However, ammonia possesses a distinct pungent odor, which facilitates easy leak detection even at very low concentrations (below danger thresholds), thus enabling early warning [32]. Its high volatility also allows ammonia gas to disperse rapidly into the atmosphere in the event of a leak, minimizing the risk of localized accumulation and explosion compared to fuels heavier than air, such as propane or gasoline [35].

The application of ammonia as a fuel for internal combustion engines faces numerous technical challenges due to its inherent physicochemical properties, such as low laminar burning velocity, high minimum ignition energy, high auto-ignition temperature, and narrow flammability limits. To facilitate the deployment of this carbon-free fuel, researchers have proposed and validated various integrated technical solutions, ranging from fuel-blending strategies and hardware system enhancements to exhaust gas treatment and safety technologies. Among these, the most prevalent and effective approach to overcome the inertness and low reactivity of ammonia is the dual-fuel strategy. This method utilizes a high-reactivity fuel acting as a combustion promoter or pilot fuel to initiate and maintain stable combustion [36-37]. In spark-ignition engines, ammonia is typically blended or co-injected with gasoline, natural gas, or ethers. The addition of hydrocarbon fuels like gasoline or methane significantly reduces ignition delay, accelerates flame propagation, and enables smoother engine operation, particularly at low and medium loads [19, 29]. Research indicates that stable combustion limits are generally achieved when the equivalence ratio (ϕ) is less than 1.5 and the ammonia volume fraction is approximately 50% during co-combustion with natural gas. Similarly, for compression-ignition engines, given ammonia's extremely low cetane number and its inability to auto-ignite under standard compression pressures, diesel, biodiesel, or dimethyl ether is employed as a pilot fuel. This pilot fuel generates high-energy initial ignition kernels, which successfully trigger the combustion of the ammonia-air mixture [38].

Beyond fuel strategies, advancements in ignition systems and combustion chamber architecture are pivotal for achieving stable combustion of pure ammonia or lean-burn mixtures. Conventional ignition systems often provide insufficient energy; thus, enhancement via technologies such as multi-spark ignition, plasma ignition (including low-temperature and transient multi-pulse plasma), or laser ignition is essential to deliver higher activation energy and broader ignition kernels [39-40]. Particularly, turbulent jet ignition (TJI) technology utilizing a pre-chamber has demonstrated superior effectiveness. TJI generates high-kinetic and thermal energy turbulent jets that are discharged into the main combustion chamber, which enhances turbulence, shortens combustion duration, and enables the combustion of ultra-lean mixtures [3]. A further variant is injecting jet ignition (IJI), which combines ammonia port injection with direct hydrogen injection into the combustion chamber to create a 'seed flame,' thereby addressing scavenging issues and heat losses associated with traditional TJI [41-42].

Engines fueled by ammonia-gasoline blends represent one of the most extensively researched configurations on spark-ignition platforms, allowing for the utilization of existing infrastructure with minimal hardware modifications. Gasoline serves as a higher-reactivity fuel for co-combustion, directly addressing the inherent low reactivity and poor ignition behavior of ammonia to stabilize the combustion process [3]. Regarding operational performance, the presence of ammonia in the intake mixture yields conflicting yet optimizable effects. Due to ammonia’s lower heating value-approximately half that of gasoline-increasing the ammonia substitution ratio typically leads to a significant rise in brake specific fuel consumption

to maintain a constant power output [29]. However, ammonia possesses an exceptionally high RON, which allows the engine to operate with significantly advanced ignition timing compared to pure gasoline operation, especially under high-load conditions. Advancing the ignition phase compensates for ammonia's slow laminar burning velocity, ensuring that peak cylinder pressure is achieved at an optimal position post-TDC, thereby improving torque and indicated thermal efficiency [16]. Experimental studies have indicated that, when ignition timing is optimized, ammonia-gasoline engines can achieve thermal efficiencies comparable to or even exceeding those of original gasoline engines at wide-open throttle conditions, thanks to better compression tolerance and reduced wall heat losses due to lower flame temperatures [19, 29].

Regarding pollutant emissions, ammonia-gasoline engines exhibit superior carbon reduction capabilities but face significant challenges concerning nitrogenous compounds. CO_2 and CO emissions decrease proportionally with the ammonia fraction introduced into the combustion chamber, due to the replacement of hydrocarbon molecules with carbon-free ones [16, 43]. However, the most critical issue is the sharp surge in NO_x emissions. Unlike traditional gasoline engines where NO_x is primarily formed via high-temperature mechanisms (thermal NO_x), in these hybrid engines, NO_x originates predominantly from the nitrogen atoms within the ammonia molecules themselves (fuel NO_x) [43]. Consequently, NO_x concentrations in the exhaust can be several times higher than those of gasoline engines, necessitating the intervention of after-treatment systems. Furthermore, ammonia slip-the release of unburned ammonia-is a major concern, typically occurring under low-load conditions, over-rich mixtures, or during misfire events, posing direct environmental toxicity [19]. Experimental results show that without a catalytic converter, NO_x emissions from ammonia engines can be 1.5 to 3 times higher than those of gasoline engines with equivalent displacement [44].

The systematic review above reveals the following unresolved challenges that define the research gap addressed by the present study: (1) Pure ammonia combustion in small-displacement high-speed SI engines remains unresolved; (2) Multi-point ignition using conventional spark plugs has not been systematically investigated; (3) Quantitative optimization of ignition configuration and timing for ammonia engines is lacking. There is not any publication in the literature that provided a systematic quantitative comparison of single-point versus multi-point ignition configurations combined with ignition timing optimization specifically for pure ammonia SI engines. Such a study is essential for establishing the design guidelines needed to develop practical ammonia-fueled motorcycle engines.

This study presents, for the first time, a systematic CFD investigation of multi-point ignition strategies for pure ammonia combustion in a small-displacement, high-speed motorcycle SI engine. By comparing single-point and three-point ignition configurations across a range of ignition advance angles at the rated operating condition of 7500 rpm, the study provides quantitative evidence that multi-point ignition using conventional spark plugs can substantially improve combustion performance - including peak pressure, heat release rate, power output, and combustion stability - without requiring fuel blending or complex ignition hardware. The findings provide practical design guidelines for the development of pure ammonia-fueled motorcycle engines as a viable zero-carbon transportation solution.

2. Material and method

2.1. Material

The research was conducted on a Honda motorcycle engine with a cylinder bore of 50 mm, a piston stroke of 55 mm, and a compression ratio of 9:1. When fueled by gasoline, the engine produces a power output of 6.4 kW at a rated speed of 7500

rpm. Upon converting to ammonia fuel, the basic engine parameters remain unchanged. As this study focuses on investigating the influence of the ignition system on the performance and pollutant emission levels of the ammonia-fueled engine, the fluid dynamics analysis is confined to the engine cylinder, excluding the intake and exhaust systems.

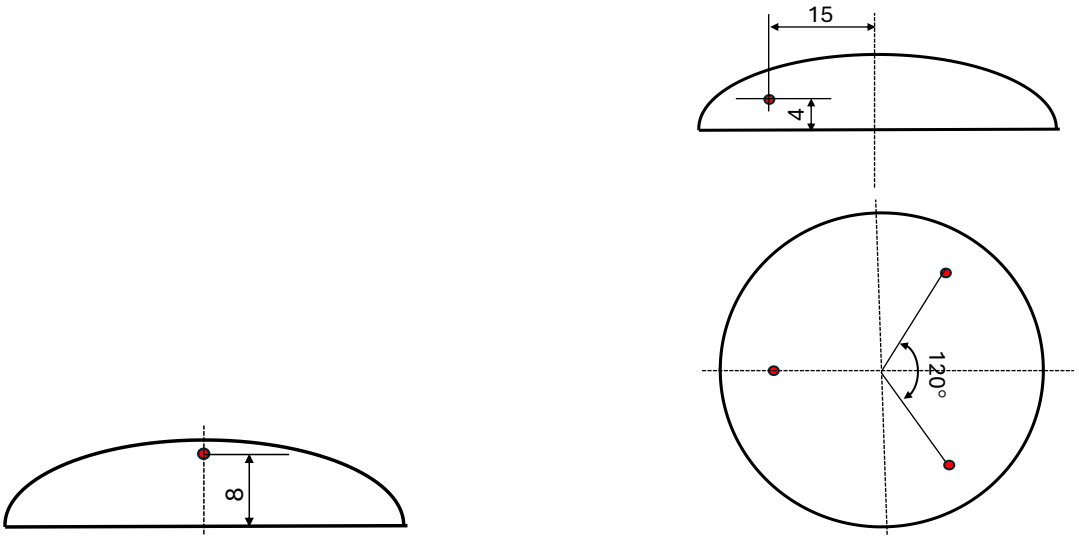

Fig. 1. Schematic of single-point (a) and three-point (b) ignition systems

Two ignition cases are analyzed in this work. In the first case, the ignition system provides a single spark via a spark plug located at the top of the combustion chamber. In the second case, the ignition system consists of three sparks equally distributed within the combustion chamber space (at 120° intervals). Fig. 1a illustrates the spark location for the first case, while Fig. 1b displays the arrangement of the sparks for the second case.

The single-point central ignition configuration represents the universal standard design for small-displacement motorcycle SI engines currently in production worldwide, including the Honda 110cc engine that serves as the platform for this study. In this configuration, a single spark plug is located at or near the center of the cylinder head, which minimizes the maximum flame travel distance to the cylinder wall (d_{max}=D/2 for the present engine). This configuration therefore already represents the geometrically optimal single-plug arrangement and serves as the most appropriate and challenging baseline against which any multi-point ignition improvement must be demonstrated.

For a circular combustion chamber cross-section, the optimal placement of nignition points that minimizes the maximum flame travel distance follows from the circle covering problem in computational geometry. For 3 sparks schema, the optimal arrangement divides the chamber into three approximately equal sectors, with the maximum flame travel distance reduced to d_{max}=D/4, a reduction of 50%.

The cylinder head of the Honda 110cc engine has sufficient space to accommodate three spark plugs at the off-center positions without requiring major structural modifications to the combustion chamber geometry or cooling passages. This practical constraint was explicitly considered in the selection of the three-point configuration.

2.2. Research Methodology

The study was conducted using the simulation method via ANSYS FLUENT software. The computational domain encompasses the engine cylinder and the combustion chamber. Fig. 2 illustrates the meshing of the computational domain when the piston is at BDC and TDC. Since the cylinder volume varies during engine operation, a dynamic mesh was applied within the cylinder

volume. The meshing method and the model establishment were described in our previous publications [45, 46, 47].

The fuel-air mixture supplied to the engine cylinder at the beginning of the compression stroke is assumed to be homogeneous. The equivalence ratio of the mixture is determined via the mixture fraction f, which depends on the fuel used. The primary component of gasoline is assumed to be C_8H_{18}. During engine operation, a portion of the lubricating oil vapor may undergo combustion, producing carbon-containing compounds. Therefore, in the case of the ammonia-fueled engine, the fuel composition is assumed to consist of 0.1% gasoline and 99.9% NH_3.

The turbulence of the gas flow within the cylinder and combustion chamber is simulated using the k-ε model. The ammonia-air mixture is assumed to be homogeneous at the beginning of the compression stroke, referring to a uniform distribution of species within the combustion chamber. This assumption is commonly adopted in CFD studies of spark-ignition engines to simplify the model and focus on the effects of ignition and combustion processes.

After ignition, turbulence plays a critical role in flame propagation, flame wrinkling, and heat release rate. Therefore, the k-ε turbulence model is employed to capture the interaction between the flame front and turbulent flow structures. The combustion process of the mixture is simulated via the Partially Premixed Combustion (PPC) model. In the present study, the ammonia–air mixture is assumed to be premixed before ignition, while turbulence-chemistry interaction governs flame propagation. Compared to other combustion models such as the Eddy Dissipation Concept (EDC) or Probability Density Function (PDF) models, the PPC model offers a reasonable compromise between computational cost and predictive capability. The EDC model is more suitable for diffusion-dominated combustion, while PDF-based models require significantly higher computational resources. Therefore, the PPC model is considered appropriate for the current study.

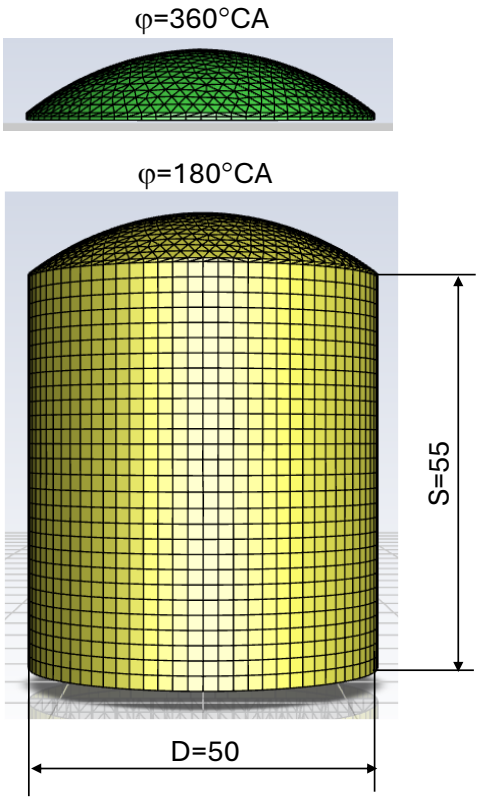

Fig. 2. Computational domain mesh at crank angles of 180°CA and 360°CA

The ammonia–air mixture is defined in ANSYS Fluent using the Species Transport framework within the Partially Premixed Combustion model. The stoichiometric combustion reaction of ammonia with air is:

$$NH_3+\frac{3}{4}O_2\rightarrow\frac{1}{2}N_2+\frac{3}{2}H_2O \quad (1)$$

The stoichiometric air-to-fuel ratio (AFR) for ammonia is 6.06 and the mixture fraction takes the value 0.1414 at stoichiometric mixture.

NOx formation is modeled using the Thermal (Zeldovich) NOx mechanism, which is the dominant NOx formation pathway at the high in-cylinder temperatures (T>1800 K) encountered during ammonia combustion. The extended Zeldovich mechanism consists of three reactions:

$$\begin{aligned} &O + N_2 \rightleftharpoons NO + N (R1)\\ &N + O_2 \rightleftharpoons NO + O (R2)\\ &N + OH \rightleftharpoons NO + H (R3) \end{aligned} \quad (2)$$

Ignition process calculations are performed using the Ignition model integrated into ANSYS Fluent software. The locations of the sparks are defined by Cartesian coordinates within the combustion chamber space. The ignition advance angle is determined before TDC. The spark energy for the gasoline-fueled engine is 0.01J. In the case of the ammonia-fueled engine, an ignition energy of 0.1J is selected to ensure the flammability of the fuel-air mixture.

The simulation is conducted during the power cycle of the engine, from the start of the compression stroke to the end of the combustion-expansion stroke. While the baseline gasoline engine was characterized across a range of operating speeds (2500, 5000, and 7500 rpm) to validate the computational framework and establish reference trends, the detailed analysis of ammonia combustion and ignition strategies is focused on the rated speed of 7500 rpm. This operating condition represents the most critical scenario for ammonia-fueled engines, as the extremely short available combustion duration (approximately 4 ms per power stroke) most severely exposes the limitations imposed by ammonia's low laminar burning velocity, and thus provides the most stringent test for evaluating the effectiveness of multi-point ignition strategies.

Table 1. Boundary Conditions

Parameter	Value
In-cylinder pressure at IVC	0.95 bar
In-cylinder temperature at IVC	340 K
Turbulent kinetic energy k_0	10 m²/s²
Turbulent dissipation rate ε_0	1000 m²/s³
Species composition	Homogeneous NH_3–air mixture at ϕ=1

3. Results and Discussion

To establish a reliable reference database for evaluating the conversion efficiency of a motorcycle engine to ammonia fuel, the performance and emission characteristics of the original engine using gasoline were first investigated. Fig. 3 presents the simulation results of the motorcycle engine during gasoline operation. The engine was operated at speeds of 2500 rpm, 5000 rpm, and 7500 rpm with corresponding ignition advance angles of φs=22˚CA,27˚CA,30˚CA under stoichiometric conditions ϕ=1. As the engine speed increases, the actual time available for ignition kernel formation, flame front propagation, and heat release decreases. Consequently, to maintain an optimal combustion phase around TDC, the ignition advance angle must be progressively increased in accordance with the engine speed.

As the engine speed rose from 2500 rpm to 7500 rpm, the ignition advance angle φ_s was adjusted from 22°CA to 30°CA BTDC. At 7500 rpm, despite the earlier spark timing, the flame front development and the heat release rate relative to the crank angle tended to lag further behind TDC (Fig. 3c).

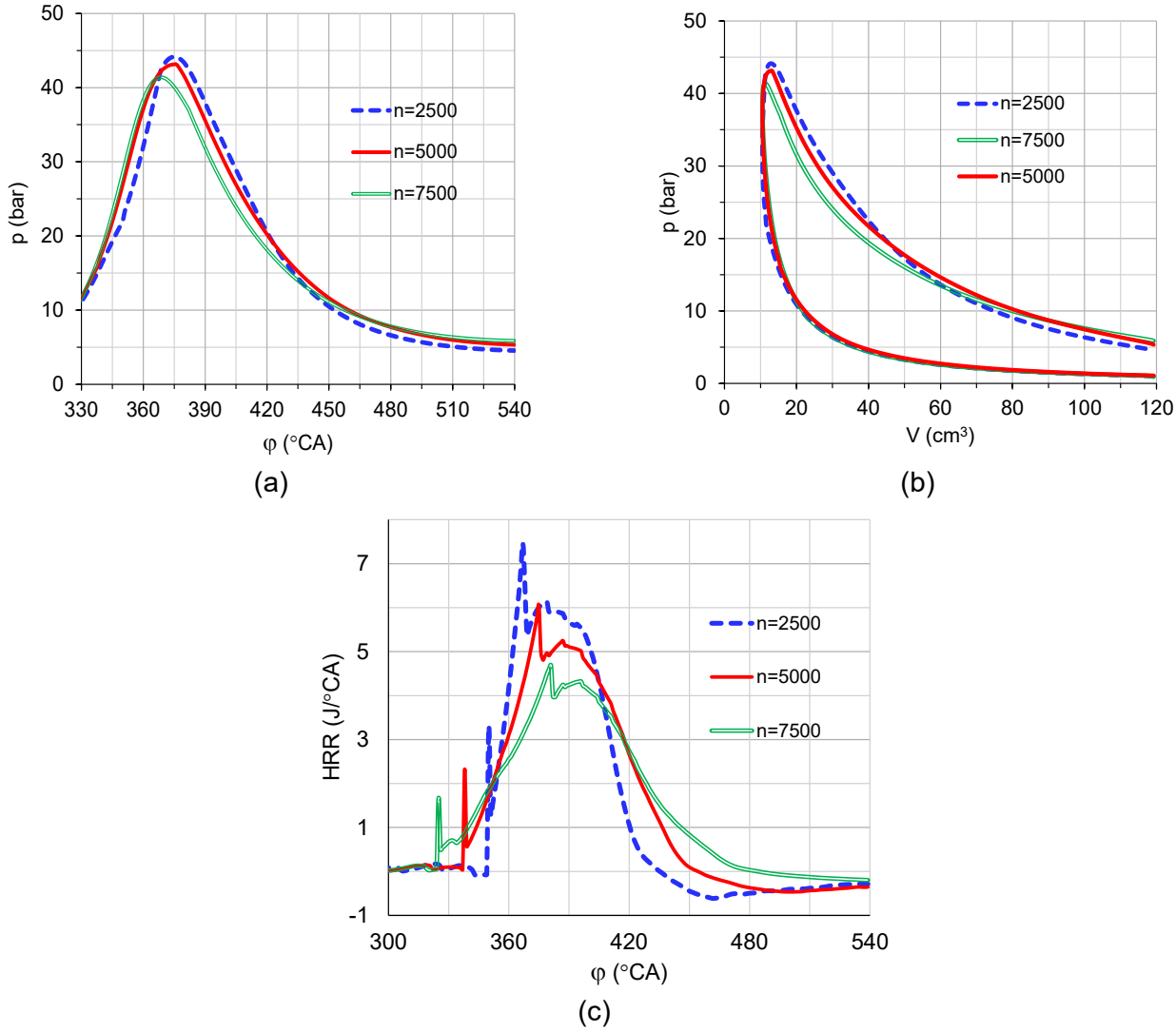

Fig. 3. Effects of engine speed on combustion pressure variation (a), P-V diagram (b), and heat release rate (c) (gasoline, wide-open throttle, ϕ=1, ignition advance φ_s=30 (n=7500 rpm), φ_s=27 (n=5000 rpm), φ_s=22 (n=2500 rpm))

This resulted in the peak cylinder pressure P_{max} failing to maintain the high levels observed at lower speeds, decreasing from 44.14 bar (at 2500 rpm) to 41.39 bar (at 7500 rpm) (Fig. 3a). This pressure decline led to a reduction in the indicated work Wi, from 135.85 J/cycle to 122.22 J/cycle (Fig. 3b).

The core reason lies in the fact that the turbulent flame speed of gasoline-although increasing with the turbulence intensity of the intake flow at higher speeds-cannot keep pace with the piston's translational speed. This affects the cycle's thermal efficiency as the heat addition process no longer retains its ideal constant-volume characteristic at TDC. This remains one of the most significant challenges for internal combustion engines operating at high speeds.

In addition to energy performance indicators, variations in engine speed profoundly influence pollutant formation mechanisms, revealing two typical contrasting trends in spark-ignition engines. Fig. 4 illustrates the formation and evolution of combustion products relative to the crank angle, reflecting the combustion completeness and thermodynamic conditions within the cylinder as speed varies. Regarding NO_x emissions, simulation results recorded a sharp decline in peak concentration from 2503 ppm at 2500 rpm to only 675 ppm at 7500 rpm (Fig. 4d). This phenomenon is entirely consistent with the Zeldovich mechanism

for thermal NO_x formation, which depends exponentially on temperature and linearly on residence time. At high speeds, although combustion temperatures remain elevated, the residence time of burned gases within the peak temperature zone is significantly shortened. This prevents NO formation reactions from having sufficient time to reach equilibrium, thereby inhibiting the NO_x generation rate.

Conversely to the NO_x trend, CO concentrations at the onset of the exhaust process increase significantly as engine speed rises, from 0.14% to 0.75% (Fig. 4a). From a chemical kinetics perspective, CO is an intermediate product vigorously generated in the primary reaction zone, which is subsequently oxidized into CO_2 during the expansion stroke if temperatures remain sufficiently high and oxygen is available. At 7500 rpm, the expansion process occurs too rapidly, causing a swift drop in burned gas temperature and shortening the window for post-combustion oxidation reactions (Fig. 4a). Consequently, the conversion of CO to CO_2 is quenched prematurely, resulting in higher residual CO in the exhaust gas. In summary, at the rated operating condition of 7500 rpm, the gasoline engine achieves a peak pressure of approximately 41.4 bar, a power output of 6.45kW, and NO_x emissions of 675 ppm. These values will serve as the benchmark parameters to for comparing and evaluating engine performance when transitioning to ammonia fuel in the subsequent analyses.

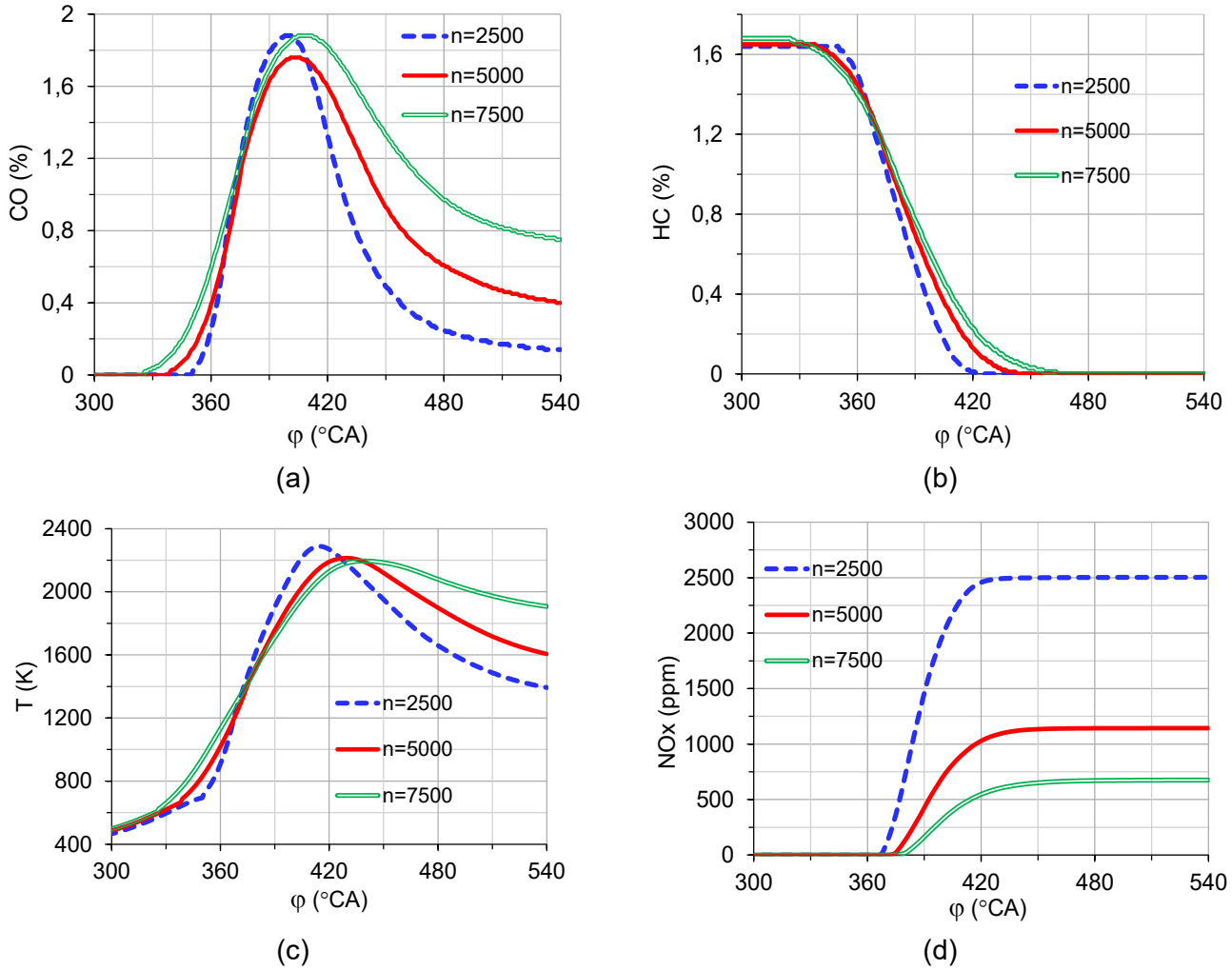

Fig. 4. Effects of engine speed on CO variation (a), HC variation (b), average in-cylinder temperature (c), and NO_x emissions (d) (gasoline fuel, wide-open throttle), ϕ=1, ignition advance φ_s=30 (n=7500 rpm), φ_s=27 (n=5000 rpm), φ_s=22 (n=2500 rpm))

3.1. Engine performance during NH_3 operation with top-center ignition

When transitioning to ammonia fuel with the original combustion chamber configuration and a traditional single-point ignition system, the engine faces severe performance challenges, particularly at the high-speed range of 7500 rpm. The core of the issue lies in the physicochemical properties of ammonia: its laminar burning velocity is extremely low, approximately 6-8 cm/s under ambient conditions, which is significantly lower than that of gasoline. Simulation results investigating the effects of ignition advance angles at 20°CA, 30°CA, and 40°CA BTDC clearly illustrate the lag of the ammonia flame front relative to the piston speed. The engine exhibits extreme sensitivity to ignition timing (combustion phasing), and the optimal operating window becomes much narrower compared to gasoline operation.

The spark advance angle - defined as the crank angle before top dead center (BTDC) at which the spark occurred - is arguably one of the most influential control parameters in SI engine operation. Its effect on engine performance can be understood through the indicated work per cycle:

$$W_{indicated}=\oint P\,dV=\int_{IVC}^{EVO} P\,dV \quad (3)$$

For maximum work output, the in-cylinder pressure should be maximized during the expansion stroke. This requires that the center of heat release (50% mass fraction burned, MFB50) occurs at a crank angle slightly after TDC, typically at 6°–10°CA ATDC for conventional fuels, where the geometric advantage of the expanding piston volume is balanced against the thermodynamic advantage of releasing heat near constant-volume conditions.

The Minimum advance for Best Torque (MBT) timing is defined as the minimum spark advance angle (i.e., the latest firing time) that produces the maximum brake torque (or equivalently, maximum indicated mean effective pressure, IMEP) at a given engine speed and load condition. It represents the optimal combustion phasing that maximizes the thermodynamic work conversion efficiency.

For ammonia, the dramatically lower laminar flame speed (S_L≈0.07 m/s, approximately 5–6 times lower than gasoline) has profound implications for MBT timing. The time required for the initial flame kernel to grow from the spark gap to a self-sustaining propagating flame is inversely proportional to the laminar flame speed. For ammonia, this flame development period is approximately 3–5 times longer than for gasoline at equivalent conditions, requiring a correspondingly earlier spark advance.

A detailed analysis of the in-cylinder pressure development (Fig. 5a) reveals that even when operating at 30°CA BTDC-considered the most optimal ignition timing among the surveyed cases-the peak pressure only reaches 41.39 bar. While numerically comparable to gasoline, the power generation process is far less efficient, resulting in a power output of only 4.36 kW. This power drop of over 30% compared to the gasoline engine (6.45 kW) indicates that a single-point ignition system alone lacks sufficient energy and spatial distribution to initiate a flame front fast enough to encompass the entire combustion chamber within the extremely short duration of the power stroke. The heat release rate diagram shows a low peak and a broad curve, indicating that the combustion process is sluggish and extends far into the expansion stroke (Fig. 5c).

When the ignition advance is reduced to 20°CA BTDC, the situation deteriorates further. At this stage, the piston begins its rapid descent, increasing the combustion chamber volume while the flame front lacks the capability to accelerate. This volumetric expansion leads to a drop in pressure and temperature (Fig. 5d), inducing a local quenching effect that further weakens the chain reaction rate. Consequently, the peak pressure plunges to approximately 30 bar, and engine power drops severely. Conversely, the

strategy of increasing the ignition advance to 40°CA BTDC to compensate for the slow burning velocity does not yield the expected results. Although peak pressure can be maintained, igniting the mixture too early while the piston is still ascending (compression stroke) generates significant negative compression work, which offsets the work produced during the expansion stroke. Furthermore, maintaining a high-pressure and high-temperature gas mass for an extended duration before TDC significantly increases heat losses through the cylinder walls and piston crown. Thus, with a single-point ignition configuration, the physical limit of ammonia's burning velocity becomes an insurmountable bottleneck that cannot be overcome by merely adjusting ignition timing, leading to low energy conversion efficiency and an inability to meet the operational requirements of motorcycle engines under high-load, high-speed conditions.

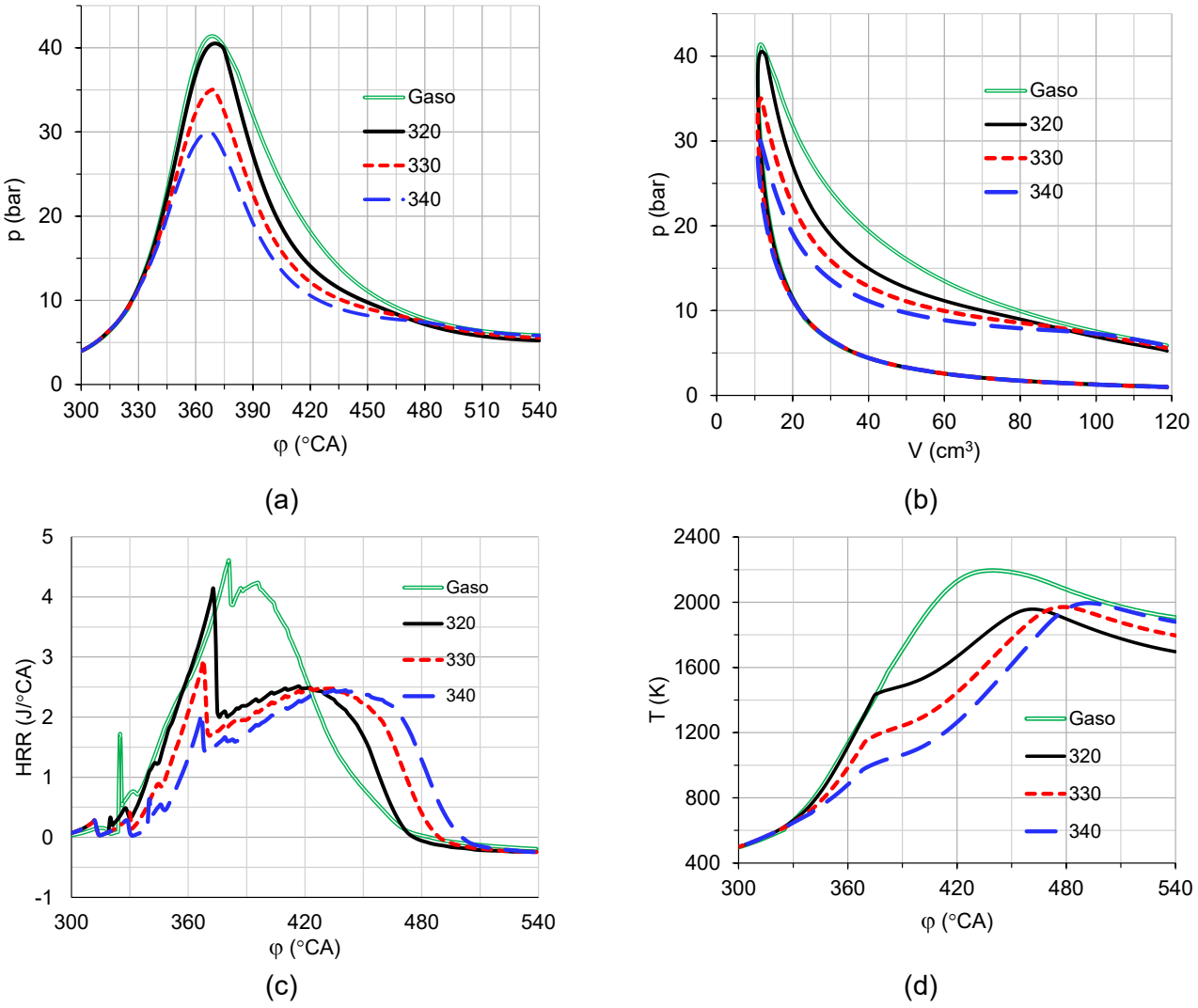

Fig. 5. Effects of ignition advance angle on combustion pressure variation (a), P-V diagram (b), heat release rate (c), and average in-cylinder temperature (d) (NH_3 fuel, n=7500rpm, ϕ=1)

3.2. Performance of NH_3-fueled engine with three-point ignition in the combustion chamber

During the compression stroke, the upward motion of the piston compresses the in-cylinder charge and simultaneously generates significant turbulent kinetic energy through squish flow - the radial outward motion of gas from the piston crown toward the cylinder wall as the piston approaches TDC. The turbulent kinetic energy kevolves according to:

$$\frac{Dk}{Dt}=\frac{\partial}{\partial x_j}\left[\left(\mu+\frac{\mu_t}{\sigma_k}\right)\frac{\partial k}{\partial x_j}\right]+G_k-\rho\varepsilon+S_k \quad (4)$$

where the production term $G_k=\mu_t S^2$(with Sbeing the mean strain rate tensor magnitude) is directly driven by the velocity gradients generated by piston motion. The simulation results show that the turbulent kinetic energy reaches its peak value near TDC, precisely at the moment of ignition, which is physically consistent with the well-established understanding of SI engine in-cylinder flow dynamics.

For ammonia combustion, the enhancement of flame propagation by turbulence is particularly critical due to ammonia's characteristically low laminar flame speed (S_L≈0.06-0.08 m/s at stoichiometric conditions and atmospheric pressure). The turbulent flame speed $S_T$predicted by the Zimont TFC closure is:

$$S_T = A \cdot u' \left(\frac{u' \cdot l_t}{S_L \cdot \alpha}\right)^{-0.25} \quad (5)$$

At the operating condition of 7500 rpm, the simulation predicts a turbulent velocity fluctuation of u'≈3.2m/s near TDC, yielding a turbulence enhancement ratio:

$$\frac{S_T}{S_L} = A \cdot \frac{u'}{S_L}\left(\frac{u' \cdot l_t}{S_L \cdot \alpha}\right)^{-0.25} \approx 8\text{–}12 \quad (6)$$

This means that turbulence amplifies the effective flame propagation speed of ammonia by approximately one order of magnitude, making turbulence–flame interaction the dominant physical mechanism enabling practical ammonia combustion in this engine. Without this turbulent enhancement, the flame front would travel at only ~0.07 m/s - far too slow to complete combustion within the available 4 ms power stroke duration at 7500 rpm.

Under the three-point ignition configuration, three flame kernels are initiated simultaneously at spatially distributed locations within the combustion chamber. Each kernel generates its own local flow divergence as the burned gas expands, creating additional velocity gradients that locally increase the turbulent production term G_k. The interaction between adjacent expanding flame fronts further enhances local turbulence intensity through flame–flame interaction zones, where converging flow fields from neighboring kernels create regions of elevated strain rate and turbulent kinetic energy. This positive feedback between multiple flame kernels and the turbulent flow field provides an additional mechanism - beyond the simple geometric reduction in flame travel distance - that accelerates heat release under the three-point ignition configuration.

Fig. 6 presents the simulation results of the in-cylinder temperature field at TDC. Three cases are compared: (a) the gasoline engine with single-point ignition; (b) the ammonia engine with single-point ignition; and (c) the ammonia engine with an evenly distributed three-point ignition system. In all cases, the engine operates at 7500 rpm with a stoichiometric equivalence ratio ϕ=1 and an ignition advance angle φ_s=30°CA. Observing the flame front development (represented by the high-temperature red zones) at TDC, the distinct differences in combustion characteristics between the fuels and ignition configurations are clearly evident.

First, for the traditional gasoline fuel (Fig. 6a), the flame front has developed vigorously with a propagation radius of approximately 10 mm from the spark plug center. The expanded combustion zone occupies a significant portion of the combustion chamber volume, ensuring a rapid pressure rise for power generation. Second, in the case of ammonia with a single-point ignition configuration (Fig. 6b), at the same timing and ignition angle, the flame front development is extremely limited, reaching a radius of only about 4 mm. This directly reflects the disadvantage of ammonia's low laminar burning velocity (which is approximately 5–6 times lower than that of gasoline), leading to a severe phase lag in the heat release process relative to the piston movement. Third, for the ammonia configuration with three-point ignition (Fig. 6c), the simulation imagery shows the simultaneous formation of three

independent ignition kernels evenly distributed within the combustion chamber. At TDC, each ignition kernel reaches a radius of about 5 mm. Although the size of each individual kernel remains smaller than in the gasoline case, the total flame front area of the three-point system is several times larger than that of the single-point ammonia case.

The improvement in combustion performance associated with the multi-point ignition strategy cannot be solely ascribed to the enlargement of the initial flame front area; it is also fundamentally governed by the complex interaction between multiple flame kernels and the in-cylinder turbulent flow field. The presence of multiple ignition sites intensifies flame–turbulence interactions, thereby enhancing flame wrinkling and increasing the effective flame surface area. This, in turn, promotes a higher flame propagation speed and reduces the overall combustion duration. Furthermore, the turbulent flow field facilitates improved fuel–air mixing and augments convective heat transfer within the combustion chamber, leading to an elevated heat release rate and enhanced combustion efficiency. A larger total flame front area implies that the mass of the mixture entrained into the reaction zone increases substantially. The results indicate that the multi-point ignition system effectively compensates for the slow burning characteristics of ammonia, accelerating the fuel consumption rate and the overall heat release rate to more closely approximate the characteristics of a gasoline engine. This successfully overcomes the power degradation typically observed at high speeds.

To address the low burning velocity of ammonia without altering the fuel composition (such as blending with hydrogen or gasoline), an improved ignition system-transitioning from single-point to three-point ignition (3 sparks) evenly distributed within the combustion chamber-is analyzed. Geometrically, the simultaneous activation of combustion at three different locations (spaced 120° apart) generates three spherical flame fronts developing in parallel. The total flame front surface area-the direct factor determining the fuel consumption rate-is multiplied from the initial stages of the combustion process. This serves as a 'physical catalyst,' effectively compensating for the inherently low laminar burning velocity of ammonia.

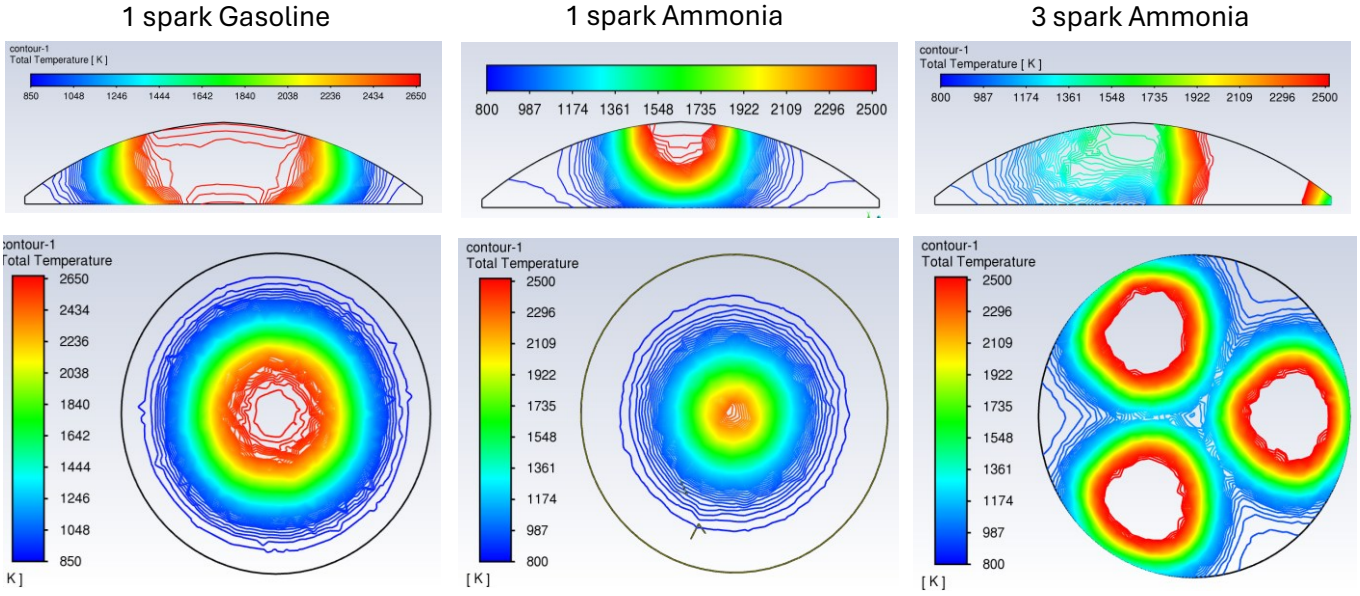

Fig. 6. Comparison of flame front development at TDC during engine operation at 7500 rpm and stoichiometric mixture conditions ϕ=1, ignition advance φ_s=30°CA: (a) Gasoline, single-point ignition; (b) Ammonia, single-point ignition; (c) Ammonia, three-point ignition

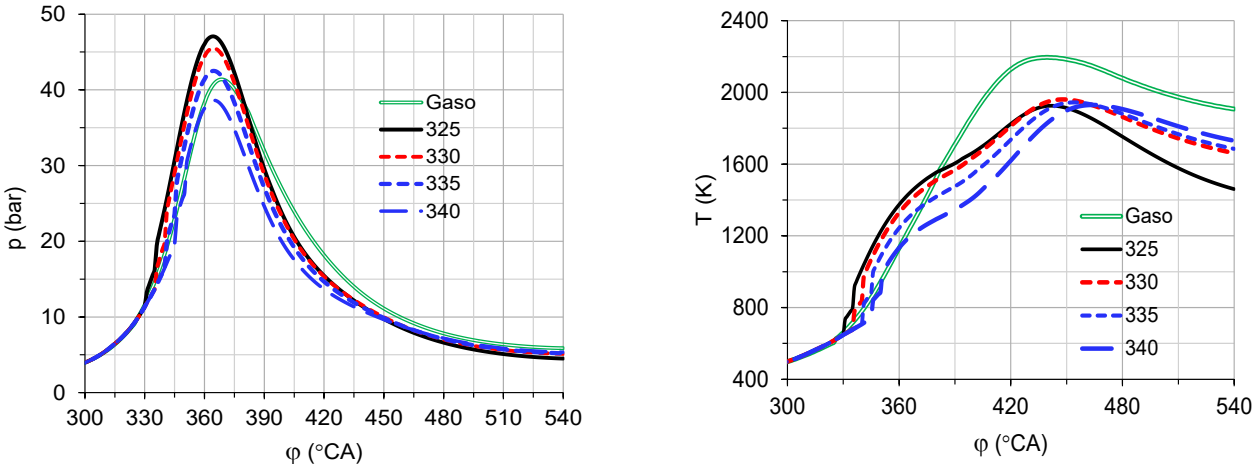

(a) (b)

Fig. 7. Effects of ignition advance angle on combustion pressure variation (a) and average in-cylinder temperature variation (b) (NH_3 fuel, n=7500rpm, ϕ=1, ignited by three evenly distributed sparks; "Gaso" represents the gasoline-fueled engine case at n=7500rpm)

The simulation results indicate that this ignition model significantly enhances the combustion characteristics of NH_3. At the same ignition advance angle of 30°CA BTDC, while the single-spark configuration only generates a peak pressure of 35.03 bar (under identical operating conditions), the three-spark system pushes the maximum pressure up to 45.49 bar (Fig. 7a). This value even surpasses the peak pressure of the original gasoline engine (41.39 bar). This demonstrates that with the support of multi-point ignition, the heat release rate of ammonia is substantially improved, allowing the majority of the fuel to be burned and its heat release to be concentrated near TDC, more closely approximating the ideal isochoric heat addition cycle. A direct consequence of this improved combustion quality is a surge in engine power from 4.36 kW (1 spark) to 5.36 kW (3 sparks) (Fig. 7b), representing an increase of approximately 23%. This marks a significant advancement in restoring the performance of engines using alternative fuels.

However, although the peak pressure of NH_3 (3 sparks) is higher than that of gasoline, the resulting power output remains approximately 16.25% lower (5.36 kW compared to 6.45 kW).

The cause of this phenomenon lies in the differences in temperature and the thermodynamic properties of the combustion products. Simulation results indicate that the maximum average cycle temperature for NH_3 only reaches about 1,960 K (Fig. 7b), considerably lower than the 2,195 K observed in the gasoline cycle. Lower temperatures equate to lower internal energy of the gas mass, thereby limiting the work-producing capability during the expansion stroke. Furthermore, the number of moles of gaseous products from ammonia combustion is lower than that of gasoline, which also contributes to the reduction in indicated work. Sensitivity analysis of the ignition angle reveals that the three-spark system helps broaden the engine's 'operating window' while ignition retarding causes a severe power drop in the single-spark configuration, the three-spark system maintains good performance even with later ignition timings at 20°CA or 25°CA BTDC. This provides great flexibility in engine control, offering more room to optimize other parameters, particularly emissions.

3.3. Comparison of pollutant emission levels between NH_3 engine with single-spark and three-spark ignition

Ammonia is a carbon-free fuel; therefore, in theory, its combustion products do not contain CO or CO_2. In practice, however, trace amounts of CO and CO_2 may still be present in the exhaust gas,

resulting from the combustion of a very small fraction of lubricating oil vapor. In this study, we assumed the NH_3 fuel contains 0.1% gasoline to simulate this practical reality.

The transition from a single-point to a multi-point ignition system not only impacts dynamic performance but also fundamentally alters the engine's emission profile, posing a classic trade-off in internal combustion engine design. First, the absolute advantage of ammonia-fueled engines regarding carbon-based emissions must be reaffirmed. In all simulation cases-whether using one or three sparks, CO and HC concentrations remained near zero (with CO at only 0.03-0.04% compared to 1.88% for gasoline) (Figs. 8a, b). These results confirm ammonia's immense potential for the complete elimination of greenhouse gases and carbon-based pollutants.

However, the primary challenge lies in the surge of NO_x emissions when applying the multi-point ignition solution. The mechanism of NO_x formation in internal combustion engines primarily follows the thermal NO_x (Zeldovich) mechanism, which is strongly governed by local peak temperatures and the residence time of combustion products in high-temperature environments. With three sparks, the combustion process is faster, more intense, and more concentrated. While beneficial for thermal efficiency, this inadvertently creates ideal conditions for NO_x formation. At the optimal operating point for power (30°CA BTDC ignition advance), the NO_x concentration for the three-spark configuration jumps to 908 ppm-nearly three times higher than the 353 ppm recorded for the single-spark configuration. This increase is the price to be paid for the accelerated burning rate and elevated combustion chamber temperatures.

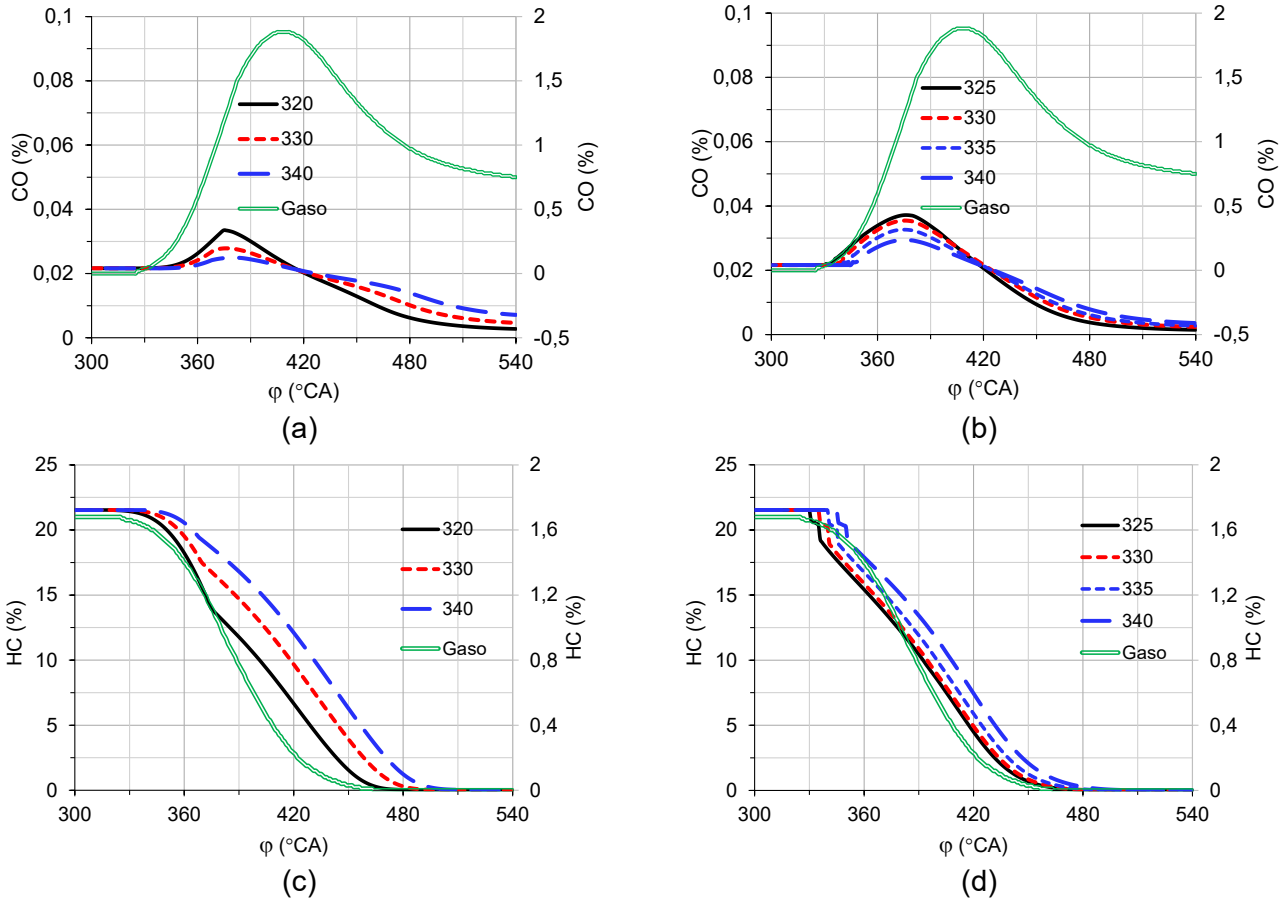

Fig. 8. Comparison of the effects of ignition advance angle on CO, HC, and NO_x emissions of the NH_3-fueled engine with single-spark ignition (a) and three-spark ignition (b) (n=7500 rpm, ϕ=1; "Gaso" represents emissions from the gasoline-fueled engine at n=7500 rpm)

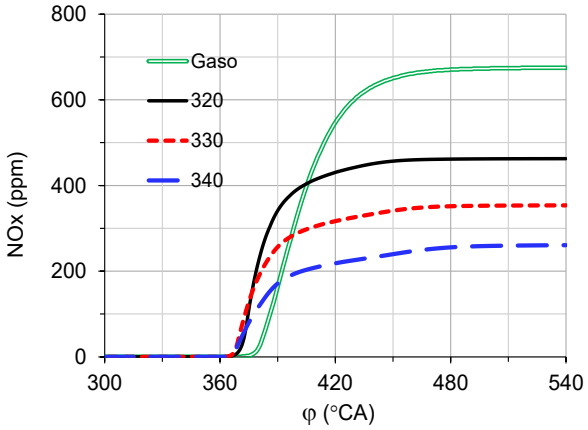

(e)

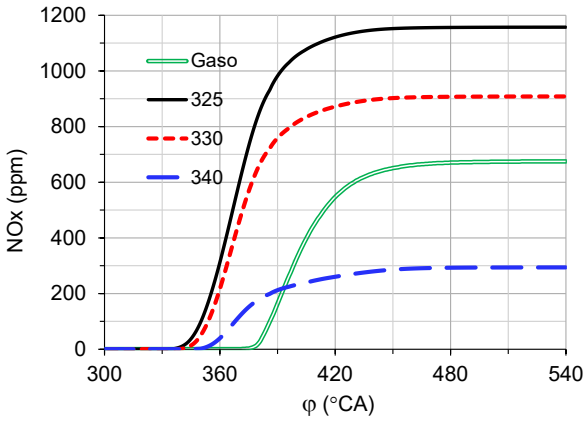

(f)

Fig. 8. (continued)

Nevertheless, the research results also point toward a promising direction to resolve this conflict through an ignition timing control strategy. Thanks to the rapid combustion characteristics of the three-spark system, we can proactively retard the ignition timing without the risk of excessive post-combustion or drastic power loss, as seen in the single-spark configuration. Specifically, by retarding the ignition angle to 20°CA BTDC (340° crank angle) in the three-spark setup, NO_x concentration drops sharply to only 294 ppm-a level comparable to, or even lower than, the single-spark case. It is noteworthy that at this 'clean' operating point, the engine power still reaches 4.83 kW, which is higher than the maximum power achievable by the single-spark configuration (4.36 kW). Thus, the multi-point ignition system is not only a solution for power enhancement but also provides an effective tool for emission control. From this, an important conclusion can be drawn: the optimal operating point for an ammonia engine is not necessarily the point of maximum power (where NO_x generation is highest), but rather the 'trade-off point'-where power is significantly improved over traditional designs while NO_x emissions are strictly controlled below allowable limits through a rational ignition retard strategy.

4. Conclusions

This simulation study has elucidated the impact of ignition system configurations on the performance and emissions of a motorcycle engine fueled by ammonia. Based on the findings, the following conclusions can be drawn:

+ The low laminar burning velocity of ammonia is the primary technical barrier for motorcycle engines operating at high speeds (7500 rpm). With a traditional single-point ignition system, the combustion process is excessively slow and prolonged, leading to low thermal efficiency. Consequently, the engine power drops significantly, reaching only about 67% of the gasoline-fueled power, even at the optimal ignition timing.

+ The configuration of three evenly distributed ignition points has proven to be an effective solution for overcoming ammonia's low burning velocity. By increasing the flame front area and the heat release rate, this system enables the peak in-cylinder pressure to surpass that of the original gasoline engine and increases the power output by 23% compared to the single-point configuration, significantly narrowing the performance gap with gasoline.

+ A trade-off exists between performance and NOx emissions when enhancing the burning rate. However, the study identified an optimal operating point at an ignition angle of 20°CA BTDC with the three-point system. At this point, the ignition retard strategy reduces NOx to low levels (comparable to the single-point configuration) while maintaining a power output higher than the maximum achievable by the single-point system.

+ Ammonia engines demonstrate an absolute advantage in greenhouse gas reduction, with CO and HC emissions nearing zero across all operating conditions. Combined with multi-point ignition to restore performance, ammonia is confirmed as a viable alternative fuel solution for motorcycles, aligned with carbon neutrality goals.

Acknowledgments

This work was supported by the Ministry of Education and Training of Vietnam through the research project “Investigation and Development of an Extended-Range Electric Motorcycle (EREM) Powered by a Hydrogen carrier fuel Engine,” Code: B2026-DNA-09.

References

[1] K. Uddeen, Q. Tang, H. Shi, F. Almatrafi, J.W.G. Turner. (2023). Combustion analysis of ammonia and methanol fuels and their blends in an optical spark-ignition engine. Book Chapter in Powertrain Systems for a Sustainable Future. 1st Edition. *CRC Press*.

[2] A. Doosti, M. Hoseinpour, M.G. Rasul, R. Karami, N.M.S. Hassan, B. Moghtaderi. (2025). A critical review on ammonia as a fuel for internal combustion engines: Is it a viable option? *Renewable and Sustainable Energy Reviews*, 222, 115964. https://doi.org/10.1016/j.rser.2025.115964

[3] P. Dong, S. Chen, D. Dong, F. Wei, M. Lu, P. Wang, W. Long. (2024). Future zero carbon ammonia engine: Fundamental study on the effect of jet ignition system characterized by gasoline ignition chamber. *Journal of Cleaner Production*, 435, 140546. https://doi.org/10.1016/j.jclepro.2023.140546

[4] S. Mashruk, H. Shi, L. Mazzotta, et al. (2024). Perspectives on NO_X Emissions and Impacts from Ammonia Combustion Processes. *Energy & Fuels*, 38(20), 19253–19292. https://doi.org/10.1021/acs.energyfuels.4c03381

[5] A. Valera-Medina, F. Amer-Hatem, A.K. Azad, I.C. Dedoussi, M. de Joannon, R.X. Fernandes, et al. (2021). Review on ammonia as a potential fuel: from synthesis to economics. *Energy & Fuels*, 35(9), 6964–7029. https://doi.org/10.1021/acs.energyfuels.0c03685

[6] A. Yapicioglu, I. Dincer. (2019). A review on clean ammonia as a potential fuel for power generators. *Renewable and Sustainable Energy Reviews*, 103, 96–108. https://doi.org/10.1016/j.rser.2018.12.023

[7] L. Kumar, A.K. Sleiti. (2024). Systematic review on ammonia as a sustainable fuel for combustion. *Renewable and Sustainable Energy Reviews*, 202, 114699. https://doi.org/10.1016/j.rser.2024.114699

[8] H. Kobayashi, A. Hayakawa, K.D.K.A. Somarathne, E.C. Okafor. (2019). Science and technology of ammonia combustion. *Proceedings of the Combustion Institute*, 37(1), 109-133. https://doi.org/10.1016/j.proci.2018.09.029

[9] Z. Liu, L. Zhou, H. Wei. (2023). Experimental investigation on the performance of pure ammonia engine based on reactivity controlled turbulent jet ignition. *Fuel*, 335, 127116. https://doi.org/10.1016/j.fuel.2022.127116

[10] R. Novella, J. Pastor, J. Gomez-Soriano, J. Sánchez-Bayona. (2023). Numerical study on the use of ammonia/hydrogen fuel blends for automotive spark-ignition engines. *Fuel*, 351, 128945. https://doi.org/10.1016/j.fuel.2023.128945

[11] T.F. Guiberti, G. Pezzella, A. Hayakawa, and S.M. Sarathy. (2023). Mini review of ammonia for power and propulsion: advances and perspectives. *Energy & Fuels*, 37(19), 14538–14555. https://doi.org/10.1021/acs.energyfuels.3c01897

[12] C. Lhuillier, P. Brequigny, F. Contino, C. Mounaïm-Rousselle. (2020). Experimental study on ammonia/hydrogen/air combustion in spark ignition engine conditions. *Fuel*, 269,

117448. https://doi.org/10.1016/j.fuel.2020.117448

[13] C. Zamfirescu, I. Dincer. (2009). Ammonia as a green fuel and hydrogen source for vehicular applications. *Fuel Processing Technology*, 90(5), 729–737. https://doi.org/10.1016/j.fuproc.2009.02.004

[14] H. Lesmana, Z. Zhang, X. Li, M. Zhu, W. Xu, D. Zhang. (2019). NH_3 as a transport fuel in internal combustion engines: a technical review. *Journal of Energy Resources Technology*, 141(7), 070703. https://doi.org/10.1115/1.4042915

[15] D.R. MacFarlane, P.V. Cherepanov, J. Choi, B.H.R. Suryanto, R.Y. Hodgetts, J.M. Bakker, F.M. Ferrero Vallana, A.N. Simonov. (2020). A roadmap to the ammonia economy. *Joule*, 4(6), 1186–1205. https://doi.org/10.1016/j.joule.2020.04.004

[16] K. Ryu, G.E. Zacharakis-Jutz, S.-C. Kong. (2014). Performance enhancement of ammonia-fueled engine by using dissociation catalyst for hydrogen generation. *International Journal of Hydrogen Energy*, 39(5), 2390–2398. https://doi.org/10.1016/j.ijhydene.2013.11.098

[17] Z. Wang, Y. Lin, Y. Wu, Y. Zhao, Y. Li, Z. Cai, J. Hu. (2025). Systematic assessment on the ammonia/gasoline combustion performance in a modern dual-fuel spark-ignition engine on different conditions. *Fuel*, 392, 134806. https://doi.org/10.1016/j.fuel.2025.134806

[18] J. Sun, Q. Tang, M. Wen, et al. (2024). Combustion characteristics and flame development of ammonia in an optical spark-ignition engine. *Fuel*, 375, 132601. https://doi.org/10.1016/j.fuel.2024.132601

[19] S. Liu, Z. Lin, Y. Qi, G. Lu, B. Wang, L. Li, Z. Wang. (2024). Combustion and emission characteristics of a gasoline/ammonia fueled SI engine and chemical kinetic analysis of NOx emissions. *Fuel*, 367, 131516. https://doi.org/10.1016/j.fuel.2024.131516

[20] H. Ishaq, C. Crawford. (2024). Review of ammonia production and utilization: Enabling clean energy transition and net-zero climate targets. *Energy Conversion and Management*, 300, 117869. https://doi.org/10.1016/j.enconman.2023.117869

[21] C. Zamfirescu, I. Dincer. (2008). Using ammonia as a sustainable fuel. *Journal of Power Sources*, 185(1), 459–465. https://doi.org/10.1016/j.jpowsour.2008.02.097

[22] S. Mukherjee, S.V. Devaguptapu, A. Sviripa, C.R.F. Lund, G. Wu. (2018). Low-temperature ammonia decomposition catalysts for hydrogen generation. *Applied Catalysis B: Environmental*, 226, 162–181. https://doi.org/10.1016/j.apcatb.2017.12.039

[23] D. Wang, C. Ji, S. Wang, J. Yang, Z. Wang. (2021). Numerical study of the premixed ammonia-hydrogen combustion under engine-relevant conditions. *International Journal of Hydrogen Energy*, 46(2), 2667–2683. https://doi.org/10.1016/j.ijhydene.2020.10.045

[24] W.S. Chai, Y. Bao, P. Jin, G. Tang, L. Zhou. (2021). A review on ammonia, ammonia-hydrogen and ammonia-methane fuels. *Renewable and Sustainable Energy Reviews*, 147, 111254. https://doi.org/10.1016/j.rser.2021.111254

[25] A. Valera-Medina, H. Xiao, M. Owen-Jones, W.I.F. David, P.J. Bowen. (2018). Ammonia for power. *Progress in Energy and Combustion Science*, 69, 63–102. https://doi.org/10.1016/j.pecs.2018.07.001

[26] J.S. Cardoso, V. Silva, R.C. Rocha, M.J. Hall, M. Costa, D. Eusébio. (2021). Ammonia as an energy vector: Current and future prospects for low-carbon fuel applications in internal combustion engines. *Journal of Cleaner Production*, 296, 126562. https://doi.org/10.1016/j.jclepro.2021.126562

[27] M.H. Hasan, T.M.I. Mahlia, M. Mofijur, et al. (2021). A comprehensive review on the recent

development of ammonia as a renewable energy carrier. *Energies*, 14(13), 3732. https://doi.org/10.3390/en14133732

[28] L.F. Alvarez, C.J. Ulishney, O. Askari, C.E. Dumitrescu. (2025). Neat ammonia use in a heavy-duty diesel engine converted to spark ignition focused on lean operation. *Fuel*, 382, 133786. https://doi.org/10.1016/j.fuel.2024.133786

[29] D.S. Flaih, M.F. Al-Dawody, M. Elkelawy, W. Jamshed, A. Abd-Elmonem, N.S.E. Abdalla, A. Amjad. (2025). Experimental and numerical study on the characteristics of gasoline engine powered by gasoline blended with water ammonia solution. *Fuel*, 387, 134333. https://doi.org/10.1016/j.fuel.2025.134333

[30] M.-C. Chiong, C.T. Chong, J.-H. Ng, S. Mashruk, W.W.F. Chong, N.A. Samiran, G.R. Mong, A. Valera-Medina. (2021). Advancements of combustion technologies in the ammonia-fuelled engines. *Energy Conversion and Management*, 244, 114460. https://doi.org/10.1016/j.enconman.2021.114460

[31] P. Dimitriou, R. Javaid. (2020). A review of ammonia as a compression ignition engine fuel. *International Journal of Hydrogen Energy*, 45(11), 7098–7118. https://doi.org/10.1016/j.ijhydene.2019.12.209

[32] Q. Cheng, A. Muhammad, O. Kaario, Z. Ahmad, L. Martti. (2025). Ammonia as a sustainable fuel: Review and novel strategies. *Renewable and Sustainable Energy Reviews*, 207, 114995. https://doi.org/10.1016/j.rser.2024.114995

[33] V. Negro, M. Noussan, D. Chiaramonti. (2023). The potential role of ammonia for hydrogen storage and transport: a critical review of challenges and opportunities. *Energies*, 16(17), 6192. https://doi.org/10.3390/en16176192

[34] S. Oh, C. Park, J. Oh, S. Kim, Y. Kim, Y. Choi, C. Kim. (2022). Combustion, emissions, and performance of natural gas-ammonia dual-fuel spark-ignited engine at full-load condition. *Energy*, 258, 124837. https://doi.org/10.1016/j.energy.2022.124837

[35] G. D'Antuono, E. Galloni, D. Lanni, F. Contino, P. Brequigny, C. Mounaïm-Rousselle. (2024). Assessment of combustion development and pollutant emissions of a spark ignition engine fueled by ammonia and ammonia-hydrogen blends. *International Journal of Hydrogen Energy*, 85, 191–199. https://doi.org/10.1016/j.ijhydene.2024.08.210

[36] Q. Huang, J. Liu. (2024). Preliminary assessment of the potential for rapid combustion of pure ammonia in engine cylinders using the multiple spark ignition strategy. *International Journal of Hydrogen Energy*, 55, 375–385. https://doi.org/10.1016/j.ijhydene.2023.11.136

[37] T. Zhu, X. Yan, Z. Gao, Y. Qiu, L. Zhu, Z. Huang. (2024). Combustion and emission characteristics of ammonia-hydrogen fueled SI engine with high compression ratio. *International Journal of Hydrogen Energy*, 62, 579–590. https://doi.org/10.1016/j.ijhydene.2024.03.035

[38] K. Ryu, G.E. Zacharakis-Jutz, S.-C. Kong. (2014). Effects of gaseous ammonia direct injection on performance characteristics of a spark-ignition engine. *Applied Energy*, 116, 206–215. https://doi.org/10.1016/j.apenergy.2013.11.067

[39] S. Abubakar, Y. Li. (2026). Ammonia-fueled internal combustion engines: a review of research trends. *Fuel*, 406, 137016. https://doi.org/10.1016/j.fuel.2025.137016

[40] B. Zhang, M. Rubio, F. Egolfopoulos, S.B. Cronin. (2025). Stable combustion of ammonia in an internal combustion engine: a single fuel approach enabled by multi-pulse transient plasma ignition. *Fuel*, 381, 133502. https://doi.org/10.1016/j.fuel.2024.133502

[41] F. Guo, J. Yu, S. Liao, Y. He. (2025). Ammonia-hydrogen combination engine with injecting jet

ignition (IJI): the concepts and ignition mechanism. *Fuel*, 402, 135977. https://doi.org/10.1016/j.fuel.2025.135977

[42] M.K. Roy, N. Kawahara, E. Tomita, T. Fujitani. (2013). Jet-guided combustion characteristics and local fuel concentration measurements in a hydrogen direct-injection spark-ignition engine. *Proceedings of the Combustion Institute*, 34(2), 2977–2984. https://doi.org/10.1016/j.proci.2012.06.103

[43] Z. Wang, C. Ji, T. Zhang, S. Wang, H. Yang, Y. Zhai, H. Wang, J. Yang. (2024). Effect of ammonia addition on combustion characteristics of hydrogen/air using passive turbulent jet ignition. *Applied Thermal Engineering*, 236, 121827. https://doi.org/10.1016/j.applthermaleng.2023.121827

[44] X. Meng, C. Zhao, Z. Cui, X. Zhang, M. Zhang, J. Tian, W. Long, M. Bi. (2023). Understanding of combustion characteristics and NO generation process with pure ammonia in the pre-chamber jet-induced ignition system. *Fuel*, 331(Part 1), 125743. https://doi.org/10.1016/j.fuel.2022.125743

[45] V.G. Bui, T.M.T. Bui, L.C.T. Nguyen, V.H. Bui, K.B. Le, Ü. Ağbulut, M.T. Duong. (2024). Flashback control in supplying onboard-produced HHO to enrich gasoline-fueled motorcycle engines. *International Journal of Hydrogen Energy*, 93, 1316-1329. https://doi.org/10.1016/j.ijhydene.2024.11.034

[46] V.G. Bui, T.M.T. Bui, V.H. Bui, M.T. Vu, L.C.T. Nguyen, T.T. Le, Ü. Ağbulut, A.T. Hoang. (2025). Mitigating backfire occurrence in HHO-gasoline plug-in hybrid motorcycle engine. *International Journal of Hydrogen Energy*, 138, 755-774. https://doi.org/10.1016/j.ijhydene.2025.05.179

[47] V.G. Bui, T.M.T. Bui, M.T. Nguyen, L.C.T. Nguyen, V.H. Bui. (2025). Analysis of combustion enhancement and GHG emission reduction in gasoline-HHO hybrid motorcycles. *Case Studies in Thermal Engineering*, 75, 107225. https://doi.org/10.1016/j.csite.2025.107225